Chin. J. Chem. Eng., **15**(4) 579—585 (2007)

Measurement and Influence Factors of the Flowability of Microcapsules with High-content *β*-Carotene*

XU Xinde(许新德)[a,b], **YAO Shanjing**(姚善泾)[a,**], **HAN Ning**(韩宁)[a] **and SHAO Bin**(邵斌)[b]
[a] Department of Chemical and Biochemical Engineering, Zhejiang University, Hangzhou 310027, China
[b] Xinchang Pharma. Factory, Zhejiang Medical Co. Ltd., Xinchang 312500, China

Abstract The flowability of five kinds of microencapsulation powders, with different *β*-carotene contents and by two alternative particle-forming technologies *i.e.* spray-drying and starch-catching beadlet technology, was measured. The actual flow properties of the five powders were compared based on bin-flow test, and three flow indexes (Hausner ratio, repose angle and flow index) were measured. It was found that the repose angle is the most suitable index to reflect the flowability of these powders for the particle properties would not be altered due to compaction or tapping during the measuring process. Particle size and particle size distribution play most important roles in the flowability of these granular materials, which was also influenced by other factors like shape, surface texture, surface roughness, *etc*. Microcapsules with wall material of gelatin and a layer of modified starch absorbed on the surface showed excellent flowabilities and good mechanical properties, and they are favorable for tabletting to supply *β*-carotene.
Keywords *β*-carotene, microcapsule powders, flowability, Hausner ratio, repose angle

1 INTRODUCTION

Carotenoids, such as *β*-carotene, have long been demonstrated to be capable of providing some medical or health benefits, including the possible prevention or treatment of skin cancer and cardiovascular disease [1—4]. Moreover, *β*-carotene is still an important biological compound for its provitamin A activity[5].

With the increasing knowledge of the positive functions of *β*-carotene, more and more people take interest in some foods or pharmaceuticals containing *β*-carotene ingredients, such as beverages, baked goods, oils, capsules and tablets. Usage of tablets made of high-content *β*-carotene granule or powder to provide this active material is very effective and conventional. Besides high-content, some properties, such as particle size, size distribution, surface texture, surface energy, moisture content, flowability, compactibility, morphology of the powder or granule, are also very important for the formation and characterization of the tablet. Among them, the flowability and compactibility are two essential factors to ensure a successful process for preparing tablets[6—8].

In recent years, there appeared some kinds of *β*-carotene powders/beadlets in the market. These products, contained different compositions or produced by different particle-formed methods, were not all fit for being compressed into a tablet. In this work, the flowability of different microencapsulated powders with high *β*-carotene content is studied to make sure which kind of *β*-carotene microcapsules is suitable for tabletting dosage. In detail, Hausner ratio, flow index and repose angle of different *β*-carotene microcapsules are chosen as three flow indexes for comparing with their actual-flow properties based on bin-flow test, so as to find the most congruent flow index to reflect its flowability. Furthermore, the reasons for the discrepancies of flowability through different indexes and factors influencing the *β*-carotene microcapsule powders flowability are also discussed.

2 MATERIALS AND METHODS

2.1 Materials

The test materials consist of five kinds of pharmaceutical or food powders with high-content *β*-carotene, in which three kinds contain 10% of *β*-carotene and the rest two content 20% of the same active ingredient. Meanwhile, they were produced by two processes—spray-drying and starch-catching beadlet technology. Spray-drier GLZ-5 was from Shanming Machine Co., Fujian, China. When particles were produced with starch-catch beadlet technology[9], the prepared emulsion was sprayed from a revolving spray head into a fluidized bed with modified starch particles operated at 0℃. After all the emulsion had been collected by the fluidized starch particles, the entire mixture was dried with air of moderate temperature, then the dried mixture was screened and the *β*-carotene-containing particles retained on the screen were collected.

Five kinds of samples were produced by Xinchang Pharma. Factory, Zhejiang Medical Co. Porcine gelatin were from Roussellet (Wenzhou, China), modified starch were supplied by National Starch&Chemical Trading Ltd., and sucrose was purchased from the local market.

The components and the operation methods of the powders as well as the main components, including its *β*-carotene content, microcapsule wall material, $D_{90\%}$, $D_{10\%}$, $D_{50\%}$ and spans of the particle sizes of five different particles were listed in Table 1.

Received 2006-05-11, accepted 2006-12-27.
* Supported by the National Natural Science Foundation of China (No.20576118) and National High Technology Research and Development Program of China (863 Program, No.2006AA02Z210).
** To whom correspondence should be addressed. E-mail: yaosj@zju.edu.cn

Table 1 The main components, drying methods and other physical properties of the five kinds of *β*-carotene microencapsulated powders

	Content of *β*-carotene	Wall material of the microcapsules	Methods of forming powder	Mean particle size, μm	$D_{90\%}$	$D_{10\%}$	$D_{50\%}$
SD-10S	10%	modified starch, sucrose	spray-drying	240.0	361.1	123.5	240.0
SD-10G	10%	gelatin, sucrose	spray-drying	115.6	180.5	17.5	114.2
SD-20G	20%	gelatin, sucrose	spray-drying	120.4	203.2	24.5	118.4
SC-10GS	10%	gelatin, starch, sucrose	spray and starch-catching beadlet technology	242.9	324.4	165.2	249.0
SC-20GS	20%	gelatin, modified starch, sucrose	spray and starch-catching beadlet technology	281.4	371.6	194.0	277.4

	Span	Sphericity (ψ)	ρ_B, kg·cm^{-3}	ρ_P, kg·cm^{-3}	Hausner ratio	Water content, %
SD-10S	0.99	0.82	335	1121	1.20	5.9
SD-10G	1.43	0.90	563	1315	1.25	7.1
SD-20G	1.51	0.92	446	1297	1.13	6.0
SC-10GS	0.64	0.95	685	1467	1.12	6.9
SC-20GS	0.64	0.95	608	1370	1.09	6.1

Note: The five kinds of powders also contain a spot of emulsion as ascorbate palmitate, anti-oxidizer vitamin E, *etc*. $D_{90\%}$ is the diameter for which 90% of the samples is smaller, $D_{10\%}$ is the diameter for which 10% of the samples is smaller, $D_{50\%}$ is the diameter for which 50% of the samples is smaller, and Span = $(D_{90\%} - D_{10\%})/D_{50\%}$. Particle density ρ_P measured by gas flow method.

2.2 Methods

2.2.1 *Particle physical properties analysis*

In order to study the surface properties of particles, scanning electronic microscopy (FEI, USA) was used. Samples were placed on a brass cylinder and coated with gold/palladium thin layer with a fine-coat ion sputter JFC1100.

Ten particles were observed by optical microscopy, fitted with a CCD monochrome camera connected to a MATROX grabbing board. The size and shape descriptors characterizing each particle as in its silhouette were calculated. Two parameters, the silhouette breadth (B, smallest dimension) and length (L, largest dimension), were noted, and the degree of sphericity ψ is defined as

$$\psi = \frac{L}{B} \tag{1}$$

Particle size and particle size distribution were analyzed with coulter LS-230 laser particle size analyzer.

2.2.2 *Descriptions of the flowability of particles*

(1) Hausner ratio

Hausner ratio (HR) is defined as[10]

$$\mathrm{HR} = \frac{\rho_{\mathrm{tapped}}}{\rho_{\mathrm{aerated}}} \tag{2}$$

where ρ_{aerated} (aerated bulk density) of a powder is determined by allowing the dispersed powders to settle in a container under the influence of gravity; ρ_{tapped} (tapped bulk density) is obtained by tapping the container mentioned above. The values of HR could distinguish the powder flowability of the free-flowing, easy-to-fluidize group from that of the cohesive, difficult-to-fluidize group.

Densities of the *β*-carotene microencapsulated powders were examined as suggested by the European Pharmacopoeia's Technical Procedure. Five runs were handled on each sample for the aerated density and the tapped density. The average values were used for the aerated and tapped bulk density, respectively.

(2) Flow index

Jenike shear cell was used for measuring the angle of wall friction[11]. The standard shear test technique[12] was used in this experiment. A flow function is a plot of unconfined yield strength (UYS) versus the major consolidating stress (MCS). It gives the stress needed for the testing microencapsulated powder flowing, and the inverse slope of each flow function was defined as the flow index. The instantaneous flow functions reflect the wall friction and the internal friction among particles. It represents the strength developed within a powder when consolidated, which must be overcome in making the powder flow. Higher flow index value indicates better flowability of powder, in the contrast, lower flow index reflects that the powder is prone to be cohesive[13].

(3) Repose angle

The traditional method for measuring static repose angle α as shown in Fig.1 is suitable for free-flowing granules but not for cohesive powders[14]. Some modified experimental apparatus was used to determine the repose angle of cohesive powders, too[15,16].

In order to measure both free-flowing and cohesive powder with the same apparatus, we framed an equipment as Fig.2, which was the assembly of a screen cover, a screen, a spacer ring, a chute attached to a vibrator of variable amplitude and a stationary funnel. The funnel was made with polished stainless steel and specially designed to be steep and glabrous enough for the purpose that no particles would aggregate in it as

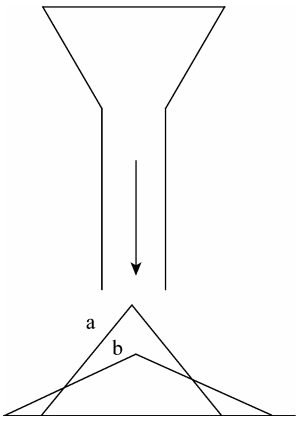

Figure 1 Repose angle for (a) cohesive and (b) non-cohesive powder

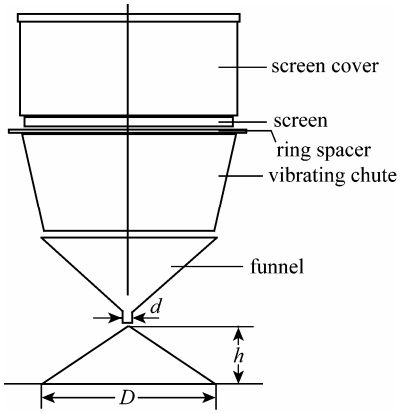

Figure 2 A repose angle tester for measuring both free-flowing and cohesive powders

they fell from the vibrating chute. Additionally, the discharging orifice is 5mm diameter and 35mm high.

The powder is poured onto the plane through the screen, the vibrating-chute, and the funnel, flowing onto a paper sheet with concentric graduated circles coaxial with the funnel orifice. The repose angle α is given by a simple geometrical construction as

$$\alpha = \tan^{-1}\left(\frac{2h}{D-d}\right) \tag{3}$$

where D and d is the diameter of the base and the orifice, respectively, and h the height of the cone of powder. Measuring the repose angle with the procedure above is straightforward and accurate for both free-flowing and cohesive powders.

Table 2 indicated the classification of flow properties with several indexes as Hausner ratio, repose angle and flow index[17].

Table 2 Classification of flowability through several indexes

	Flow index	HR	α
non flowing	＜2	＞1.4	＞60
cohesive	2—4	＞1.4	＞60
fairly free-flowing	4—10	1.25—1.4	45—60
free-flowing	＞10	1—1.25	30—45
excellent flowing	＞10	1—1.25	10—30
aerated	＞10	1—1.25	＜10

(4) Bin-flow test

A specific device assembling of an electronic balance, a vibrating bin separated by a dividing plate, modified with Zenz and Othmer's bin-flow tester[18], as shown in Fig.3, is used to manifest particle flow behavior. In the middle of the divider (ϕ150mm), there is a round opening (ϕ20 mm), which can be shut and opened by a metal slide. The whole bin, made with polished stainless steel, is tied down with a tapping machine, which would be helpful to powder flow, especial for the cohesive powders.

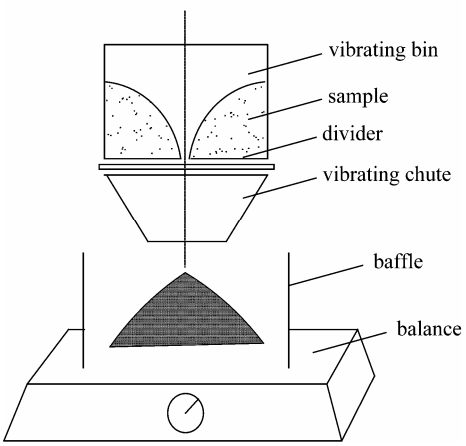

Figure 3 The bin-flow tester

In the experiment, first filling the above chamber with certain mass powders as the slide shut, then vibrating began and the slide opened, powder flow is initiated. The data from the electronic balance, which reflect the mass of falling powders, are recorded every second. Then the falling mass per flow time, that is, flow rate, is acquired. Apparently, the flow rates, including instantaneous and cumulative flow rate, reflect the relative flowability of different samples. The bin-flow test provides a "real check" for particle flowability. Here, the time required for per 100g samples falling on the balance was used to describe the flowability of different powders macroscopically.

3 RESULTS AND DISCUSSION

3.1 Physical properties

The physical properties of five food microcapsule powders were summarized in Table 1. These five samples had some similar physical properties, such as water content, which ranged from 5.9 to 7.1, and sphericity, which was around 0.90. All five β-carotene products were relatively dry sphere-shaped powders, which could be demonstrated by the scanning electronic microscopy (SEM) images in Figs.4(a)—(e). From these photos, both sample SD-10G and SD-20G have smooth surfaces and greater sphericity and some solid bridges were formed between individual microcapsules [Figs.4(a) and (b)]. These solid bridges would be adverse to the flow properties of microencapsulated powders[19].

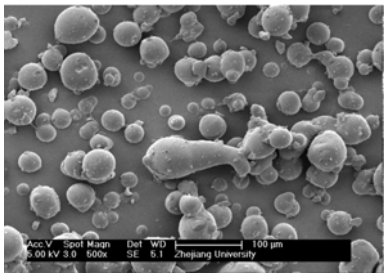

(a) SD-10G

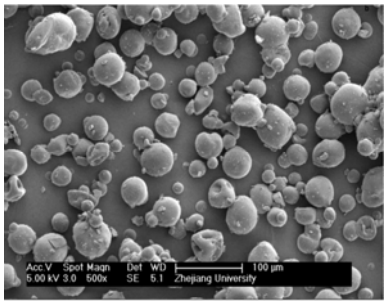

(b) SD-20G

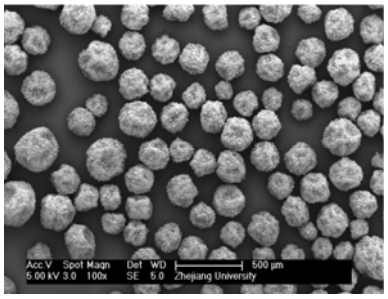

(c) SC-10GS

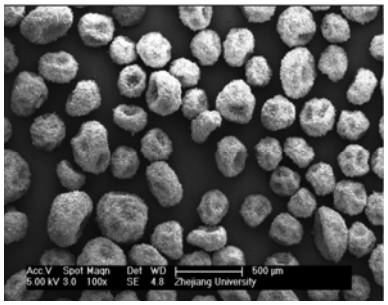

(d) SC-20GS

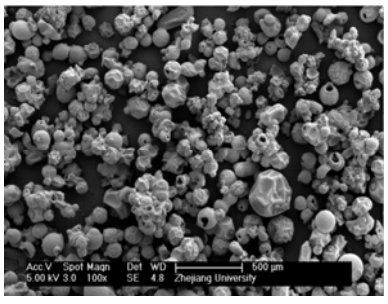

(e) SD-10S

Figure 4 Scanning electronic microscopic images of the outer surface of five kinds of *β*-carotene microencapsulated powders

The microcapsules of SC-10GS and SC-20GS [Figs.4(c) and (d)], characterized by the absorption of modified starch, had some dents but were free of pores or cracks on the outer surface, and their sphericity is both as high to 0.95. Additionally, some investigators suggested that dents were formed by shrinkage of the particles during drying and cooling[20,21].

Besides dents and cracks, there were some pores in the outer surfaces of microcapsules of SD-10S [Fig.4(e)], which also led to lower density (Table 1). The porous surfaces may be caused by the brittleness of the dry skins formed by modified starch according to the viewpoint of Rosenberg and Kopelman[22]. Meanwhile, solid bridges were common in the case and powder agglutination was formed, too. It could be concluded that the microcapsules with gelatin wall would have higher degree of integrity and less porosities on the outer surface than those with modified starch as wall material do when *β*-carotene was the core material.

The experimental results of particle size and particle size distribution of the five kinds of products were showed in Fig.5. Both mean particle sizes of SD-10S and SC-10GS were around 240μm, while that of SC-20GS was a little larger in 281.4μm. Additionally, their particle size distributions were analogous, too. The distribution of SC-20GS, SC-10GS and SD-10S were not broad, so these powders were relative homogeneous in size. While SD-10G and SD-20G microcapsules had very broad size distribution, in some parts, they had bimodal distribution. Their size span reached to 1.43 and 1.51, respectively, significantly larger than those of SD-10S (0.99), SC-10GS and SC-20GS (both 0.64). What's more, their mean sizes were 115.6 and 120.4μm respectively, much smaller than 200μm. As mentioned before, the diversity of the particle size and size distribution may result from the different composition and drying technology.

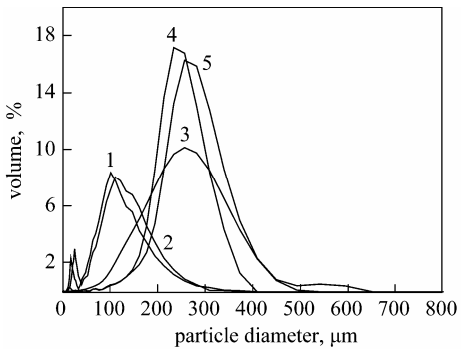

Figure 5 The particle size distribution of five kinds of *β*-carotene microencapsulated powders
1—SD-10G; 2—SD-20G; 3—SD-10S;
4—SC-10GS; 5—SC-20GS

3.2 Flow properties

As described in subsection 2.2, three indexes—Hausner ratio (HR), repose angle, flow index, were used to distinguish flowability of the five *β*-carotene microencapsulated powders. Table 3 shows the values of the three indexes and the "actual flowability" reflected

Table 3 The Hausner ratio, repose angle, flow index, bin-flow test and the flowabilities of five kinds of β-carotene microencapsulated powders

Samples	HR value	Flowability according to HR	Repose angle value, (°)	Flowability according to repose angle	Flow index (FI)	Flowability according to flow index	Bin-flow, $s\cdot(100g)^{-1}$	Reality-flowability according to bin-flow test
SD-10G	1.25	free-flowing	70.4	cohesive	2.5	cohesive	31.4	cohesive
SD-20G	1.13	free-flowing	63.9	cohesive	3.1	cohesive	27.5	cohesive
SD-10S	1.20	free-flowing	35.3	free-flowing	3.5	cohesive	8.0	free-flowing
SC-10GS	1.12	free-flowing	30.0	free-flowing	12.2	free-flowing	5.7	free-flowing
SC-20GS	1.09	free-flowing	30.0	free-flowing	11.4	free-flowing	6.3	free-flowing

from bin flow tests. Disparate conclusions about the flowability of different experimental materials could be conducted with different indexes. For example, judged by the Hausner ratio value, all the five powders are free-flowing, while on the analysis of flow index, samples of SD-10G, SD-20G and SD-10S are all cohesive but powders SC-10GS, SC-20GS have free-flowing property. Only the flow properties based on repose angle, which reveals that both SD-10G and SD-20G are cohesive and the other three samples are free-flowing, is in line with the real flowability according to the bin-flow test. Different results disclose that to the specific β-carotene microcapsule powders, some indexes for flowability may be not effective. It is necessary to scrutinize the theory and handling process of different flowability index.

3.2.1 *Hausner ratio*

Hausner ratios of the five samples were all less than 1.25, which was the critical point of free-flowing. It's obvious that, according to HR value, powders SD-10G and SD-20G have free-flowing instead of cohesive properties revealed by actual flowability. Similar discrepancies between HR results and real flow situations were reported[23].This is because that, addressing real particles, a number of factors must be taken into account when investigating the tapped bulk density.

For powders like SD-10G and SD-20G, having an almost bimodal size distribution, tapping may result in a significant volume reduction because it allows the particles to reorient. In other words, the smaller particles would fill in the interspace between larger particles. Hence, it would lead to a high tapped bulk density and sequence a high HR. However, in practice it is not in this case because HR value of SD-10G and SD-20G were 1.25 and 1.13, respectively. It may be the reason that the wall materials of both microcapsules were gelatin containing a certain amount of sucrose, and the particle surface was very cohesive and rather hard. Furthermore, the particles have a reasonable sphericity [Figs.4(a) and (b)]. So the initial aerated bulk density was already quite tightly packed and there is little room for rearrangement and consolidation which is responsible for local deformation. Then the tapped bulk density was not significantly higher than the aerated bulk density, which lead to a small HR. So the conclusion of powder flow properties suggested by Hausner ratio of SD-10G and SD-20G is not correct characterization.

3.2.2 *Flow index*

Figure 6 reveals the instantaneous flow functions of the five powders. Compared the classification of flowability by flow index with the conclusion of bin-flow tests(Table 2), the only difference is the flowability of SD-10S, which is free-flowing in actual check.

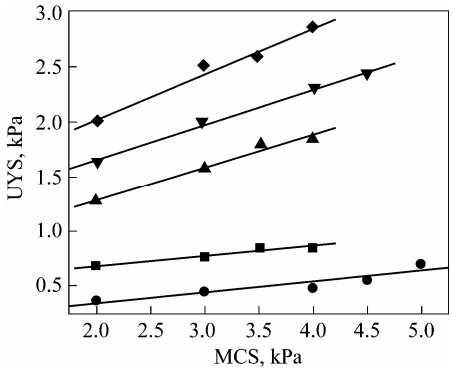

Figure 6 The flow functions of five kinds of β-carotene microencapsulated powders
■ SC-20GS; ● SC-10GS; ▲ SD-10S; ▼ SD-20G; ◆ SD-10G

The flow function reflects the surface force interactions from one powder to another. These interactions can be categorized as internal friction and cohesive forces. Now it can be known that cracks and dents would certainly increase the friction, and cohesive forces is mainly van der Waals forces, or even chemical bonds, or capillary forces associated with liquid bridging[24]. For the five powders, in which the water contents were relatively low, there was no liquid bridging shown in the SEM images. In this case, the cohesion mainly means van der Waals force or/and chemical bonds.

Besides the properties of particle surface and its interactions, the particle size is also important for the flow function. Smaller particle size, which would probably provide a greater surface area for interparticle cohesive forces to interact, will probably result in more cohesive flow.

Among the five powders, with compositions as gelatin and sucrose, both SD-10G and SD-20G have small particle size and a small quantity solid bridge

between particles. As a result, their flow functions values became larger. Then for the powders of SC-10GS and SC-20GS, with larger particle size and low van der Waals forces or/and chemical bonds between particles because of more starch sticking to the outer gelatin surface, would not necessarily appear to cohesive. For the microcapsules powder SD-10S, as mentioned above, there are many dents, cracks, pores, and even solid bridge interparticles, which would make the internal friction rise to a high level. Moreover, because of the brittleness resulted from many pores in intraparticles, under certain consolidating stress, it is possible that some particle would fall into pieces, or some angular particles would appear, which, in turn, would increase the internal frictions. So the flow function of SD-10S would be high, which lead to the result that it was cohesive instead of free-flowing described in bin-flow test. It also could predict that SD-10S powder would not be suitable to be compressed into a tablet because of its low yield stress and deformation rate. Similar conclusion was also drew when studied the flowability of ascorbic acid crystals for direct tabletting[25].

The reason why Hausner ratio of SD-10S appeared low may be that not enough outer energy was input to make the powder collapse in the tapping test according to the standard method. And if more energy input, particles would break up, too[16].

3.2.3 *Repose angle and bin-flow*

The repose angle acquired from the repose angle tester revealed in Fig.2 could describe easily and straightforwardly the flowability of the five β-carotene microcapsules powders. As shown in Table 3, the flow properties according to repose angle are in accordance with those reflected from the bin-flow test. It is that powders of SD-10G and SD-20G are cohesive while powders of SD-10S, SC-10GS and SC-20GS have free-flowing properties.

In the process of testing repose angle, no compaction and tapping manufacture were involved, which resulted in little deformation or fraction of particles. The evaluations could accurately reflect the surface properties, including the degree of coarse, particle shape, friction and cohesive forces between particles. Then, the repose angle could be used as an actual and instantaneous index of the flowability of these β-carotene microcapsule powders.

The cumulative masses and images of powders flowing from a vibrating bin onto a balance at noted time internals in the bin-flow experiment, as shown in Fig.7, illustrate the flow pattern and flow rate of different powders.

It can be found from Fig.7 that samples of SC-10GS, SC-20GS and SD-10S flow quickly and their flow rates are almost invariable, while SD-10G and SD-20G exhibits localized disruptions in flow rate. Because the latter are cohesive, their flow patterns are not uniform[26]. For the same reason, these two powders would not flow down to the balance without importing energy through vibration. The intermittent flows also indicate that their cohesive forces and frictions between particles are much larger than those of

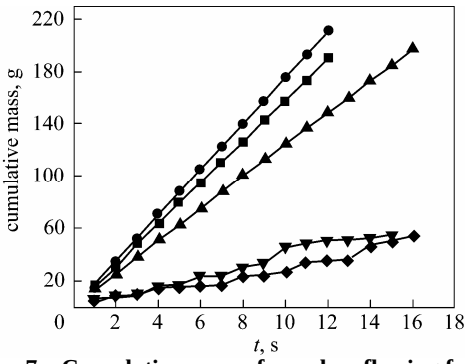

Figure 7 Cumulative mass of powders flowing from a vibrating bin onto a balance at noted time intervals in the bin-flow experiment
■ SC-20GS; ● SC-10GS; ▲ SD-10S; ▼ SD-20G; ◆ SD-10G

SC-10GS, SC-20GS and SD-10S. It means that the former two powders are cohesive while the latter three have free-flowing properties.

3.2.4 *Factors of influencing the powder flowability*

Flowability is actually dependent on the attraction between particles, including friction and adhesion. Interparticle friction mostly depends on the characteristics of outer surface of particles, which is in turn determined by the ingredient of the wall material and the preparation method to form the particles. Generally speaking, smoother surface results in smaller friction, while interparticle adhesion is caused by intermolecular forces, including van der Waals forces, local chemical bonds, electrostatic charges, and bridging forces.

Besides chemical compositions, particle size and size distribution are other two very important factors to determine particle flow property. Particle size influences contact area greatly. For bigger particles, gravity is generally greater than interparticle adhesive force, making the flow easier. The relation between particle gravity and interparticle adhesive forces and its influence on the particle flowability were well-discussed by Li *et al*.[27]. Small quantity of fine particles in larger particles would lead to good powder flowability because of the lubricating ability. However, too many small granules would increase the contact area. Additionally, a broad particle size span will make the contact area larger and the flow more difficult. So the wide particle distribution, including the bi-modal pattern, would do harm to the flow properties of pharmaceutical powders[15].

The samples of SC-10GS, SC-20GS and SD-10S, whose mean particle size is all larger than 240μm, display free-flowing feature according to the criteria of repose angle or the bin-flow test. Moreover, that the sample of SD-10S, despite of the existed solid-bridge between particles, aggregation because of the great interparticle adhesive forces, and the poor sphercity, shows good flowability, demonstrates that particle size plays a very important role in particle flow property, which is in accordance with some conclusions drawn from some investigations on the flowabilities of other food particles[15,16,27].

Powders like SD-10G and SD-20G, having perfect sphericity and smooth outer surface(Fig.4), but also having relative large interparticle adhesive force and small mean particle size around 120μm and a broad size distribution, as shown in the bin-flow test, were still difficult to flow.

4 CONCLUSIONS

Hausner ratio and flow index, measuring particle flowabilities indirectively, may be deceptive or misleading. In the case of no compaction and tapping, that is, no external forces are imposed to make particles deformation during the process of manufacture, and the repose angle is an instantaneous and easy way to measure the particle flowability.

For spray-drying technology, when used gelatin and sucrose as capsule wall material, the particles, such as SD-10G, SD-20G, with large interparticle adhesion forces will show low flowabilities. On the other hand, when using modified starch as wall material, no matter how good flow property the particles have, because of the cracks, pores, dents in the outer surface, and solid-bridge between particles, they are not fit for compressing into tablets, too. When starch-catching technology was applied, the microencapsulated powder, for example, SC-10GS and SC-20GS, with gelatin and sucrose as wall materials, absorbed a layer modified starch on the outer surface and showed perfect flowability and good mechanical properties, seemingly suitable for producing tablet.

REFERENCES

1 van Pope, G., "Review: Epidemiological evidence for β-carotene in prevention of cancer and cardiovascular disease", *Eur. J. Clin. Nutrit.*, **50**, 557—561 (1996).
2 Base, A., van den Berg, H., van der Plas, R.M., "β-Carotene as antioxidant", *Eur. J. Clin. Nutrit.*, **50**, 554—556(1996).
3 Nicol, M., Maudet, M., Savoure, N., "Commented publication: About the A.T.B.C. Finland study", *Med. Nutrit.*, **30**, 212—217(1994).
4 Blumberg, J., Block, G., "The α-tocopherol, β-carotene cancer prevention study in Finland", *Nutrit. Rev.*, **52**, 242—245(1994).
5 Osleb, J.A., "Provitamin A function of carotenoids, the conversion of β-carotene to vitamin A," *J. Nutrit.*, **119**, 105—108 (1989).
6 Guerin, E., Tchoreloff, P., Leclerc, B., Deleuil, M., "Rheological characterization of pharmaceutical powders using tap testing, shear cell and mercury porosimeter", *Int. J. Pharm.*, **189**, 91—103(1999).
7 Beach, E.R., Tormoen, G.W., Drelich, J., "Pull-off force measurements between rough surfaces by atomic force microscopy", *J. Colloid Interface Sci.*, **247**, 84—99(2002).
8 Rabinovich, Y.I., Adler, J.J., Ata, A., "Adhesion between nanoscale rough surfaces Ⅰ role of asperity geometry", *J. Colloid Interface Sci.*, **232**, 10—16(2002).
9 Harade, E., Morikawa, K., "O/W emulsion and process for producing food with the same", Jpn. Pat., WO 2004/062382 (2004).
10 Hausner, H., "Friction conditions in a mass of metal powder", *Int. J. Powder Metall.*, **3**(4), 7—13(1967).
11 Jenike, A.W., "Storage and flow of solids", Eng. Exp. Stat. Bull., No.123, Univ. Utah, Salt Lake City (1986).
12 Akers, R.J., "The certification of limestone powder for Jenike Shear Testing CRM116", Commission of the European Communities (EESC-EEC-EAEC), Brussels-Luxembourg (1992).
13 Fitzpatrick, J.J., Barringer, S.A., Iqbal, T., "Flow property measurement of food powders and sensitivity of Jenike's hopper design methodology to the measured values", *J. Food Eng.*, **61**, 399—405(2004).
14 Augenstein, D.A., Hogg, R., "An experimental study of the flow of dry powders ever inclined surfaces", *Powder Technol.*, **19**, 205—215(1978).
15 Santomaso, A., Lazzaro, P., "Transition to movement in granular chute flows", *Chem. Eng. Sci.*, **56**, 3563—3573(2003).
16 Abdullah, E.C., Geldart, D., "The use of bulk density measurements as flowability indictators", *Powder Technol.*, **102**, 151—165(1999).
17 de Jong, J.A., Hoffmann, A.C., "Finkers, properly determine powder flowability to maximize plant output", *Chem. Eng. Progr.*, **25**, 34(1999).
18 European Pharmacopoeia Commission, European Pharmacopoeia 4, Pharmaceutical Technical Procedures, Flowability, Council of Europe, Strasbourg, 208(2002).
19 Mathlouthi, M., Roge, B., "Water vapour sorption isotherms and the caking of food powders", *Food Chem.*, **82**, 61—71(2003).
20 Kalab, M., "Scanning electron microscopy of diary products: An overview", *Scanning Electron Microscopy*, **3**, 261(1979).
21 Buma, J.J., Henstra, S., "Particle structure of spray dried milk products as observed by scanning electron microscopy", *Neth. Milk Dairy J.*, **25**, 75(1979).
22 Rosenberg, M., Kopelman, I.J., "A scanning electron microscopy study of microencapsulation", *J. Food Sci.*, **50**, 139—144(1985).
23 Schussele, A., Bauer-Brandle, A., "Note on the measurement of flowability according to the European Pharmacopoeia", *Int. J. Pharm.*, **257**, 301—304(2003).
24 Ulusoy, U., Yekeler, M., Hicyelmaz, C., "Determination of the shape, morphological and wettability properties of quartz and their correlations", *Minerals Eng.*, **16**, 951—964(2003).
25 Kawashinma, Y., Imai, M., Takeuchi, H., "Improved flowability and compactibility of spherically agglomerated crystals of ascorbic acid for direct tabletting designed by spherical crystallization process", *Powder Technol.*, **130**, 283—289(2003).
26 Hickey, A.J., Comcessio, N.M., "Descriptors of irregular particle morphology of powder properties", *Adv. Drug Deliv. Rev.*, **26**, 29—40(1997).
27 Li, Q., Rudolph, V., Weigl, B., Earl, A., "Interparticle van der Waals force in powder flowability and compactibility", *Int. J. Pharm.*, **280**, 77—93(2004).